PROCEEDINGS OF SCIENCE

SuperKEKB and Belle II Status Report

Riccardo de Sangro[*†]
Laboratori Nazionali di Frascati dell'INFN
E-mail: riccardo.desangro@lnf.infn.it

After the first turn-on that occurred at the beginning of 2016, followed by a five-month single beam operation phase, the new SuperKEKB *B* Factory is presently under commissioning at the KEK laboratory in Japan. The new collider construction is now completed and it is scheduled to deliver the first e^+e^- collisions in the first half of 2018, opening a new era in the arena of physics at the high intensity frontier. We present in this paper the preliminary results of the first single beam commissioning and describe the Belle II detector upgrade. We will then describe the performance improvements obtained, and present the status of the final phases of the detector assembly and commissioning.

The 15th International Conference on Flavor Physics & CP Violation
5-9 June 2017
Prague, Czech Republic

[*]Speaker.
[†]Representing the Belle II Collaboration

PoS(FPCP2017)037

1. Introduction

In the past decade the KEKB and PEP-II B-Factory experiments *BABAR* [1] and Belle [2] have dominated the high energy physics scene with a wealth of measurements of unprecedented precision that have put the Standard Model (SM) of the weak interaction with three generation of quarks and leptons, together with the Cabibbo-Kobayashi-Maskawa mixing mechanism of *CP* violation, to a stringent test. This enormous effort of over ten years by the two international collaborations has been documented in the "Physics of the B-Factories" book [3].

Despite the overwhelming evidence of the validity of the SM, and the remarkable precise confirmation of the CKM mechanism obtained from most of the performed measurements, in a few cases the experimental results showed $2 \div 3$ standard deviations from the precise theoretical predictions. Significant examples are the measurement of the ratio $R(D^*)$ of B decays to $D^{*\pm}\tau^{\mp}\bar{\nu}_{\tau}$ [4, 5] and the angular analysis of $B \to K^*\ell^+\ell^-$ decays [6, 7]. In the last few years this picture has been further confirmed by many high precision measurements made by the LHCb experiment at CERN, in some cases enhancing the combined significance of the discrepancies [8] in others introducing new ones, like a hint of lepton flavor violation in the measurement of the ratio $R(K^{*0})$ of the branching ratios of $B^0 \to K^{*0}\mu^+\mu^-$ and $B^0 \to K^{*0}e^+e^-$ recently reported [9].

It is well known that the SM is not sufficient to explain several of nature's observed features, like the baryon asymmetry in the universe, the mass and flavor hierarchy of the quarks and leptons, the finite neutrino masses, the nature of the dark matter and dark energy which make up 95% of our universe, among others.

The next generation B Factory experimental program [10] faces the challenging task of taking on the legacy of the B Factories, improving on the high precision flavor physics measurements achieved by *BABAR* and Belle experiments, with the ambitious goal to find new physics phenomena that might answer some of these fundamental questions.

2. SuperKEKB accelerator

The KEKB accelerator has reached the world record peak luminosity for an e^+e^- collider of $2 \times 10^{34} cm^{-2} s^{-1}$. To reach the full physics potential of the Belle II physics program, the SuperKEKB accelerator has been designed [11] to exceed this already exceptional performance by a factor of 40, which required a leap in the conceptual design of the machine and represents a real technical challenge.

A completely novel approach to obtain high luminosity in a collider has been adopted, the so called "nano-beam" scheme, originally proposed by P.Raimondi for the SuperB design [12]. Machine physicists express the luminosity of an e^+e^- collider with the following formula:

$$\mathscr{L} = f_{coll} \frac{n_1 n_2}{4\pi\sigma_x\sigma_y} \tag{2.1}$$

The idea is based on the drastic reduction of the beams vertical size at the interaction region, σ_y in eq. 2.1, down to an unprecedented value of ~ 50 nm (a few hundred atomic layers!). This value is a factor of 20 smaller than the conventional design of the B Factories, and leads to an equal gain in peak luminosity. The additional factor of two needed to reach the desired overall factor of 40 is

Table 1: Summary of the most relevant SuperKEKB machine parameters compared to those of the original KEKB design and to those actually achieved.

Parameter	KEKB Design	KEKB Achieved	SuperKEKB Design
Energy (GeV) (LER/HER)	3.5/8.0	3.5/8.0	4.0/7.0
β_y^* (mm)	10/10	5.9/5.9	0.27/0.30
β_x^* (mm)	330/330	1200/1200	32/25
ε_x (nm)	18/18	18/24	3.2/5.3
$\frac{\varepsilon_y}{\varepsilon_x}$ (%)	1	0.85/0.64	0.27/0.24
σ_y (μm)	1.9	0.94	0.48/0.62
ξ_y	0.052	0.129/0.090	0.09/0.081
σ_z (mm)	4	6/7	6/5
I_{beam} (A)	2.6/1.1	1.64/1.19	3.6/2.6
$N_{bunches}$	5000	1584	2500
Luminosity ($10^{34} cm^{-2} s^{-1}$)	1.0	2.11	80

obtained by doubling the beam currents, the factor $f_{\rm coll} n_1 n_2$ in eq. 2.1. In Table 1 we summarize the most relevant SuperKEKB design machine parameters, compared to those of KEKB.

To achieve the new design parameters the KEKB accelerator complex was upgraded in almost all its components; in the cartoon in Fig. 1(a) we show the SuperKEKB accelerator, highlighting in color the new or upgraded components. These include: the replacement of short dipoles in

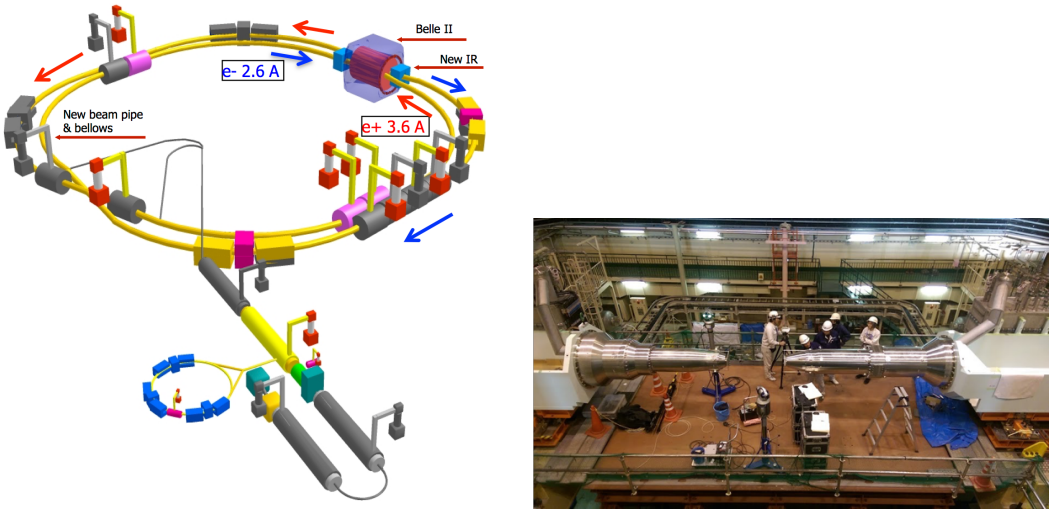

(a) (b)

Figure 1: Left: cartoon showing in color the components of the SuperKEKB accelerator complex that are new or have been upgraded from KEKB. Right: Two final focus magnets being installed on the SuperKEKB beam line.

the Low Energy Ring (LER) with longer ones; a completely new, Titanium coated beam pipe with ante-chamber; a complete redesign of the lattice for both the LER and High Energy Ring (HER); a new positron source, a new low emittance gun for the electrons and a damping ring all

to obtain extremely low emittance beams; the RF system was modified and new RF stations added for the increased beam current and finally a completely new, extremely complex, super-conducting final focus (FF) with permanent quadrupole magnets near the interaction point was designed. The construction of all these components is now complete and the commissioning of the new dumping ring will start at the end of 2017. A major milestone was achieved in winter of 2017 with the delivery of the second final focus magnet; in Fig. 1(b) we show the two facing FF magnets while they are being installed on the SuperKEKB beam line.

2.1 Commissioning status and plans

The commissioning of the SuperKEKB accelerator has been divided in two distinct phases. The first one, completed in June 2016, was carried out without the Belle II detector in the beam line; beams were circulated in both the LER and HER, but they were never collided. The second one is foreseen to start in January 2018 with the Belle II detector rolled in the beam line, but without the vertex detector that will be installed before the start of the physics run.

In the first phase, a system of radiation detectors collectively called BEAST II has been placed on the beam line in lieu of the real detector in order to measure the background generated by the circulating beams; during the second phase the BEAST II detectors will be placed in the volume left empty by the Belle II vertex detector system.

After turn-on, positron and electron currents have been circulating in the two rings almost continuously with increasing intensity for the whole commissioning period. In Fig. 2, we show a plot of the beam currents and integrated charge as a function of time. As it can be seen, a maximum current of 1010 (870) mA was achieved for the LER (HER) after about four months of running, a much faster ramp up compared with that achieved during the first commissioning of KEKB. This excellent result shows that all the upgraded hardware in the rings worked fine and that the experience gained with the operation of KEKB over past years was a key ingredient to success.

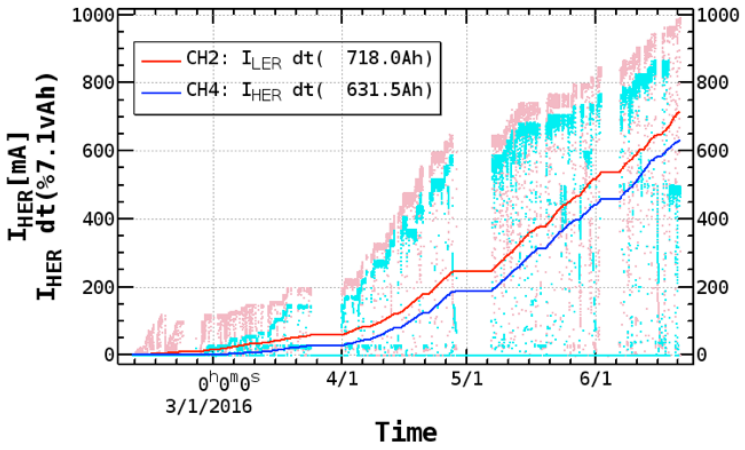

Figure 2: Initial commissioning of the SuperKEKB rings. The plot shows the circulating HER and LER currents and the total integrated charge over the four months of commissioning in spring of 2016.

The first commissioning phase of SuperKEKB had multiple goals: clean the beam pipe (vacuum scrubbing), monitor the beam conditions in real time, tune the accelerator optics, collimators

position, as well as to isolate possible sources of beam loss and collect data for beam orbit simulations useful to improve the machine performances. The effect of scrubbing the beam pipe with high circulating currents is evident in Fig. 3(a) where we show the lowering of the pressure in the beam pipe measured by sensors located in the machine arcs as a function of the integrated current. This result was confirmed by the observation of lowering background rates recorded by the BEAST II detectors in the same period of time, as shown in Fig. 3(b).

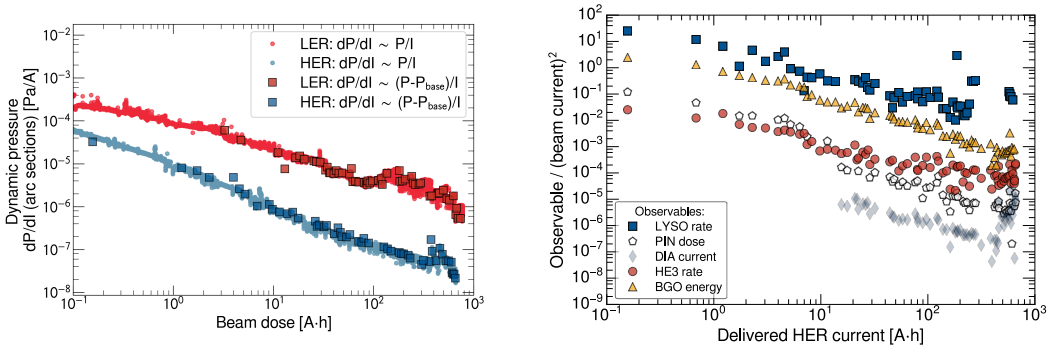

(a) (b)

Figure 3: (a) The plot shows the dynamic pressure dP/dI measured by sensors located in the machine arcs as a function of the integrated current. (b) A plot of the rate observed in various BEAST II detectors as a function of integrated dose over the same period of time confirms the improved vacuum conditions.

From the Belle II detector point of view, the goal of commissioning phase-1 was to use the BEAST II detectors to collect beam background data to validate the Monte Carlo simulations of the beam backgrounds in the detector, test a beam abort system based on diamond sensors and generally make sure there is a safe environment for operating the Belle II apparatus.

To be able to detect neutron, gamma and X ray radiation as well as charged tracks, BEAST II included several complementary sub-detectors: a PIN diode radiation monitor system; a single crystal diamond radiation detector system; a system of CsI, CsI(Tl) and LYSO crystals to measure neutral and charge electromagnetic energy; an electron and gamma radiation monitoring system based on BGO crystals; a system of scintillator tiles read out by silicon photo-multipliers, called CLAWS; a thermal neutrons detection system based on ^3He proportional tubes; a fast neutrons detector system based on four independent TPC chambers; a scintillator based system named QCSS, to record charged background near the final focus quadrupoles cryostat.

During the five months of phase-1 commissioning, BEAST II has operated recording data with all its sub-detectors; for brevity, we report here just a few examples of the preliminary results.

In the absence of beam collisions, the main sources of backgrounds in phase-1 were Touschek scattering and beam interaction (mainly Coulomb scattering) with the residual gas in the vacuum beam pipe. Touschek interactions are directly proportional to the square of the beam current and inversely proportional to the beam transverse size, whereas beam gas interactions are directly proportional to the beam current, the atomic number Z and residual pressure P of the gas species in the vacuum beam pipe. To describe the observed background rates we can thus adopt an heuristic model whereby a background related observable is given by a linear combination of the two most important components: $\mathscr{O} = B \cdot IPZ_e^2 + T \cdot \frac{I^2}{\sigma_y}$, where B and T are constants that must be extracted

from the data to represent the beam-gas and Touschek relative abundance; Z_e is an effective atomic number of the different residual atomic species in the vacuum, P the pressure in the machine, I the beam current and σ_y the transverse beam size. One example of such observable, in this case the counting rate in the BGO crystals obtained during 15 different runs taken at different beam sizes and currents, is shown in Fig. 4. Plotting $\mathscr{O}/IPZ_e^2$ as a function of $I/PZ_e^2\sigma_y$, we see that the data, as predicted by our heuristic model, lies nicely on a straight line whose intercept is the constant B, and whose angular coefficient is the constant T.

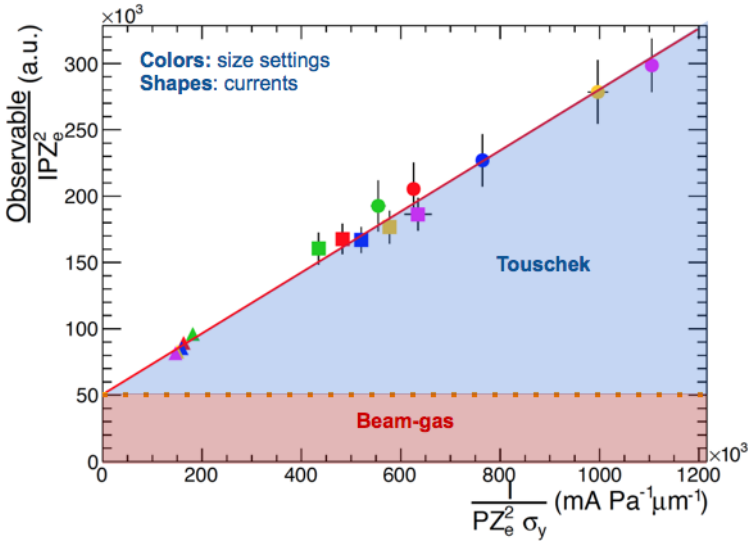

Figure 4: Plot of the background rates in the BEAST II BGO crystal system as a function of $I/PZ_e^2\sigma_y$

A detailed comparison of these data with the prediction of the Monte Carlo simulations is ongoing.

BEAST II provided relevant information about the background related to injection. During the operation of SuperKEKB, continuous beam injection is foreseen to occur at a rate of 100 Hz. During injection, the electrons' orbit parameters in the injected bunch are perturbed so as to cause an excess of particle loss, thus background radiation, in the detector. This kind of background is very difficult to simulate, therefore a measurement is necessary in order to make sure that the excess radiation does not damage the various Belle II sub-detectors.

The injection background was studied with the CLAWS, the CsI, CsI(Tl) and LYSO crystal and the QCSS systems. In Fig. 5(a) we show for example the rate in CsI crystals recorded in the first 5 ms after injection; as the data show, injection results in an increase in the background level of about 2 to 3 order of magnitude higher than that before injection. The hit rate decays back to the level pertaining to coasting beams within the first millisecond after the injection. Crystals data also show, see Fig. 5(b), that the backgrounds are highly correlated in time with the injected bunch time of passage at the interaction point ($\sim 0.75\ \mu s$, in this particular case). Knowledge of this timing structure is crucial to be able to implement a DAQ vetoing scheme able to reduce the background while keeping the dead time to an acceptable few per cent level. A paper with the results of a full analysis of the BEAST II data is in preparation and will be published soon.

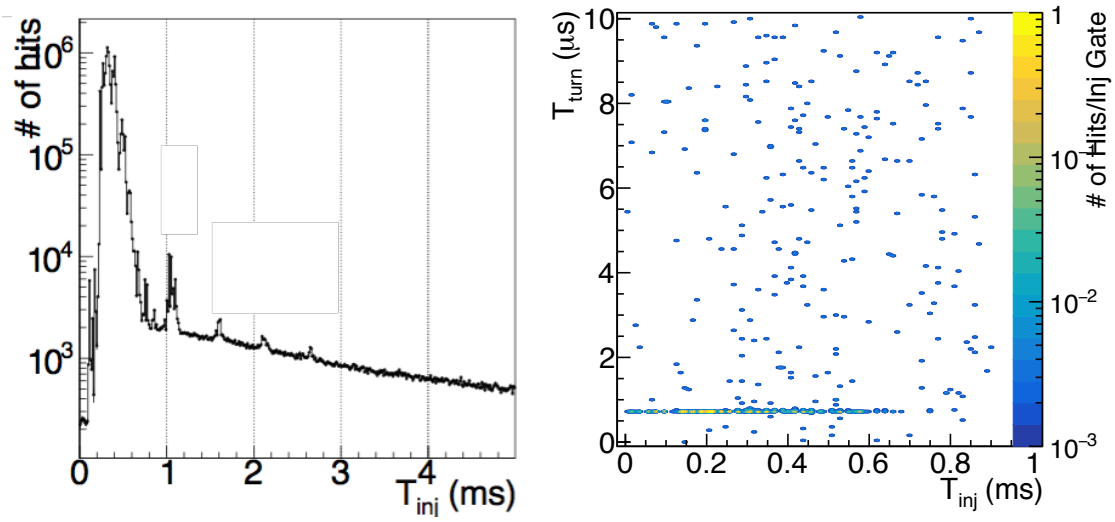

(a) (b)

Figure 5: (a) Injection background rates recorded in the BEAST II CsI crystals system as a function of time after injection, T_{inj}. The injection causes an immediate surge of the background level of $2 \div 3$ order of magnitude, which decays $\sim$1 ms thereafter. (b) plot of the time of passage of the bunches at the IP T_{turn} as a function of the time after injection, showing that the background hits are highly correlated with the time of passage of the injected bunch at $\sim$0.75 μs.

3. Belle II detector

The increase of a factor of forty in peak luminosity of SuperKEKB has several consequences: much higher occupancies in the detector leading to increased pile up and fake hits; increased trigger and data acquisition rates; possible radiation damage from the machine and physics backgrounds.

The Belle II detector design, which is based on the existing Belle detector, was thus driven by the necessity to cope with all of these problems. As a result, most of the old Belle detector components, notably the innermost ones, have either been upgraded or completely rebuilt; only the Belle solenoid, the barrel K_L and muon identifier (KLM) and the electromagnetic calorimeter CsI(Tl) crystals, have been reused. In Fig. 6 we show the Belle II detector in the top half of the picture as compared to the old Belle detector in the bottom half; in color the parts that have been changed.

Belle II is a detector with better performances overall, despite having to operate in a much harsher environment, with respect to that of Belle. In brief, it will have improved π^0 reconstruction, 30% higher K_S efficiency, better interaction point and secondary vertex resolution ($\sim$ x2); better K/π separation with a π fake rate decrease of $\sim$ x2.5; an improved electromagnetic calorimeter readout electronics which will preserve its excellent resolution in a high pile-up environment. In the following, we will present the status of the various subdetectors.

3.1 Tracking system: vertex detectors and central drift chamber

One of the most significant improvements of the Belle II detector is its tracking system. The Belle 4-layer silicon vertex detector has been replaced by a two layer, 10 million channels, silicon

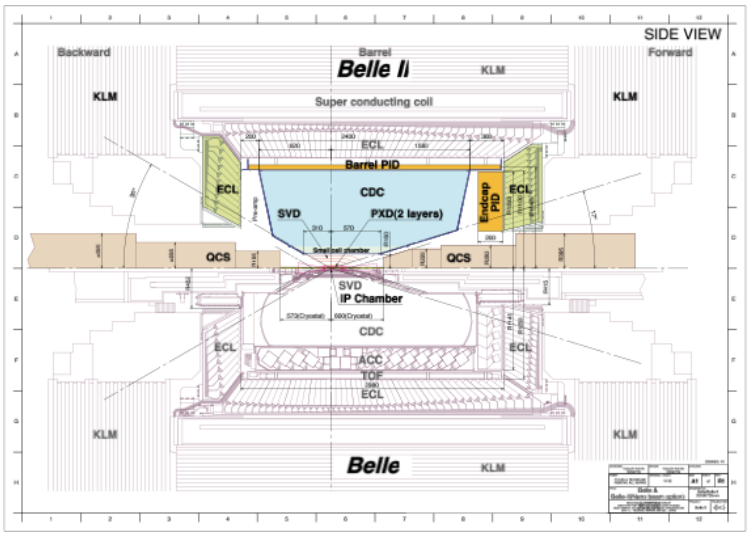

Figure 6: Belle vs Belle II detectors. In the top half of the drawing a side view of the Belle II detector is shown, with new or upgraded components are shown in colors. In the bottom half is the old Belle detector.

pixel detector (PXD) [13], followed by a 4-layer double sided silicon strip detector (SVD) [14]. The new vertex detector system, thanks to the reduced radius of the new Berillium beam pipe made possible by superKEKB nano beam scheme, has its first layer located at $\sim$12 mm radius from the interaction point and provides an impact parameter resolution of $\sim 20\mu$m. Recently a complete wedge of the PXD and SVD detectors has been assembled and exposed to a test beam at DESY, Hamburg, with all the final read out components and data acquisition chain in place. The test was very successful, in particular a major milestone was reached with the positive test of the Region of Interest (ROI) algorithm running online; this is needed to reduce the data trasfer bandwidth by identifying and reading out only the pixel that are found to be associated to SVD tracks extrapolated back to the PXD detector planes. In Fig. 3.1 we show a picture of the PXD and SVD assembly on the test beam line. The vertex detector system is on schedule to be installed on the Belle II detector during the summer of 2018, after the second commissioning phase starting in January 2018.

Belle's central drift chamber (CDC) [15] has been replaced by a new one with a much larger tracking volume, thanks to the space gained by replacing the old aerogel and time of flight barrel particle identification system (PID), with the much thinner quartz bars of the new PID system. The 14,000 sense wire, 56-layer (32 axial + 24 stereo) CDC provides a spatial resolution of $\sigma_{r\phi}$=100μm, σ_z=2 mm and a momentum resolution, when combined with the SVD, of $\sigma_{p_t}/p_t = \sqrt{(0.1\%p_t)^2 + (0.3\%\beta)^2}$.

The CDC construction has been completed; in Fig. 8(a) we show the transverse resolution obtained analyzing cosmic ray data taken after the installation inside the solenoidal magnet. In Fig. 8(b) we show the combined IP resolution as a function of p_t using as input the latest simulation obtained using the most recent results from cosmic ray or test beam data. It is interesting to note that, despite the boost of SuperKEKB is lower than that of KEKB (a factor of 28/44), yet Belle II's Δt resolution is better that of Belle, as $\sigma_{\Delta t}^{BelleII} \sim 0.75\ \sigma_{\Delta t}^{Belle}$.

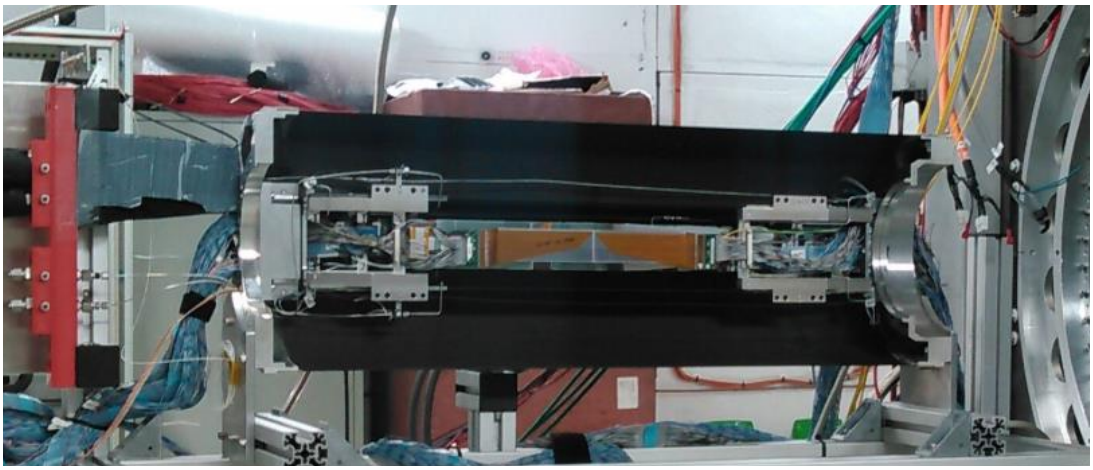

Figure 7: Picture of a fully equipped complete wedge of the PXD+SVD vertex detector system assembled on a DESY test beam line.

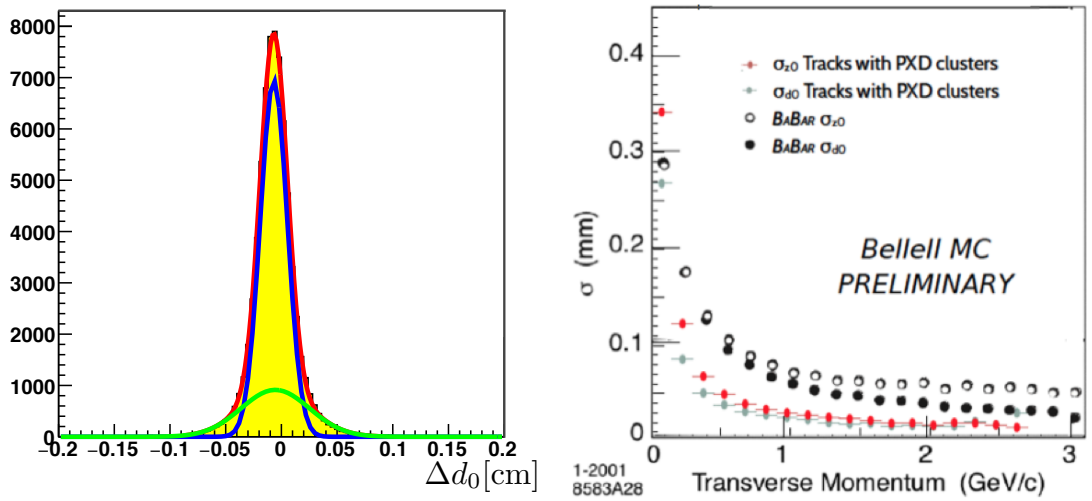

(a) (b)

Figure 8: (a) Plot of the CDC transverse resolution performances using cosmic ray data; the resolution is well modeled with two Gaussian. (b): Plot of the combined vertex resolution as a function of p_t obtained with the most recent simulation in which all the latest results from real detector performances measured using test beam or cosmic ray data are used as input.

3.2 Time Of Propagation: TOP

The Belle aerogel Cherenkov detector in the barrel has been replaced by the more compact Time Of Propagation detector [16]. The system is based on the collection of Cherenkov light emitted by the charged particles traversing a quartz bar. The light propagates through the bar via multiple internal reflections and is collected at one end by a light guide that concentrates the photons on an array of multi-anode photo-multipliers, while it is reflected by a mirror at the other end. In Fig. 9 we show a picture of a quartz bar with light from a test laser propagating inside it. The different Cherenkov light emission angle causes the photons to take different light paths

in the bar and thus to have different times of propagation from the impinging track position to the light detectors. The discrimination of different particle species is based on the extremely precise measurement ($\sim$100 ps) of this time of propagation, as can be seen from the plots in Fig 10.

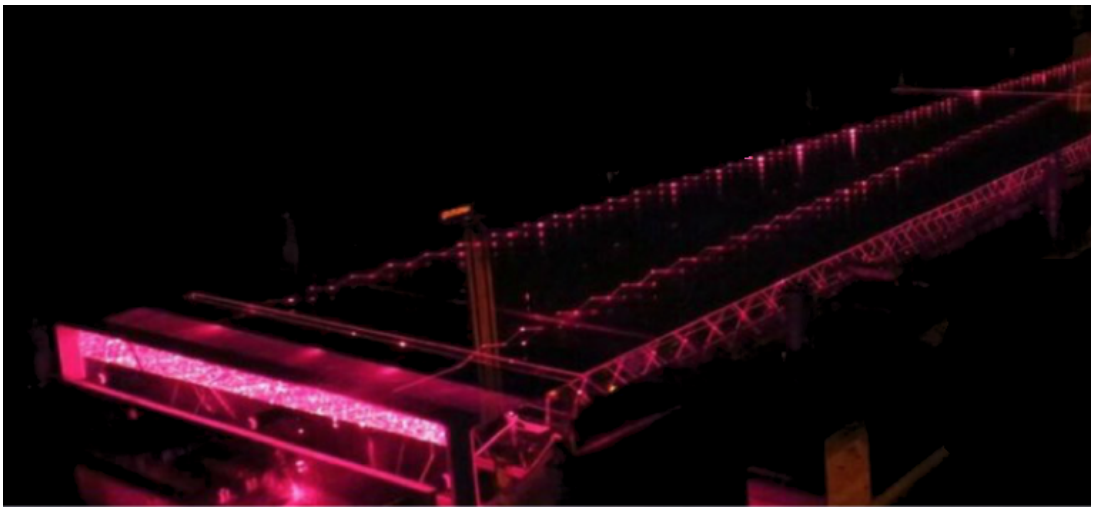

Figure 9: Picture of one of the 16 quartz bars of the TOP detector. One can see the light from a laser beam propagating throughout the bar with multiple reflections.

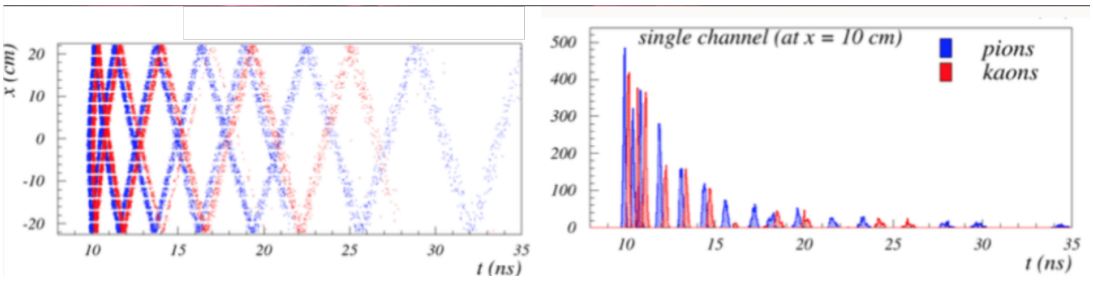

Figure 10: Plot showing the time of arrival of light signals collected by one channel of the multi-anode PMT. Photons from pions and kaons have different arrival times and can thus be discriminated.

The TOP includes 16 quartz bars surrounding the central drift chamber; they are all installed inside the Belle II detector and taking cosmic ray data.

3.3 Aerogel RICH

In the forward direction a new proximity focusing aerogel RICH particle identification system was designed and built [17]. Two aerogel layers of different refraction index in focusing configuration allow to increase the number of photons without resolution degradation, see Fig. 11(a). Cherenkov photons are focused on a plane where an array of Hybrid Avalanche Photo Diodes are placed to detect them. The system has been built, fully instrumented and test beam data showed that the desired K/π separation, while keeping π misidentification probability below few percent, can been obtained over the desired momentum range (Fig. 11(b)); The ARICH is now ready to be installed on the detector (Fig. 12).

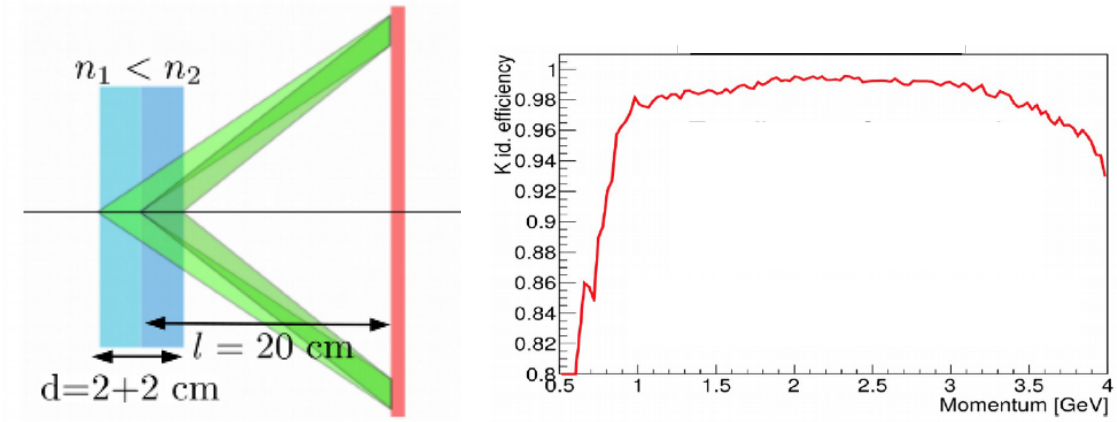

(a) (b)

Figure 11: (a) Principle of operation of the proximity focusing aerogel detector: two consecutive layers of aerogel have refraction index chosen so as to cause the Cherenkov light to be focused on the photon detectors plane. (b) Test beam data shows excellent K/π separation, for 2% of π misidentification probability, over a large momentum range.

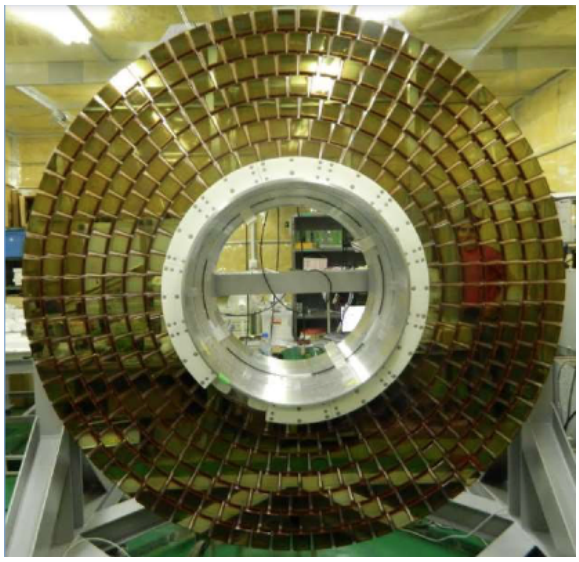

Figure 12: The fully assembled A-RICH is ready to be installed on the Belle II forward endcap.

3.4 Electromagnetic calorimeter ECL

The Belle electromagnetic calorimeter consists of 8736 Thallium-doped CsI crystals, and will be used unchanged by the Belle II experiment (Fig. 13). However, to cope with the higher level of background expected while operating at SuperKEKB, the readout electronics has been upgraded [18]. In addition to a shorter signal shaping time, a digital signal processing (DSP) module has been added to the readout chain in order to record signal waveforms with 1.76 MHz sampling frequency. The waveforms are then fitted, and the time and amplitude extracted, directly online. Early prototypes were tested on the Belle backward endcaps; we show in Fig. 14(a) that with the old electronics (blue circles) the equivalent noise energy σ_{noise} increases, in the presence of increasing

pile-up from background, by a factor of ∼2; thanks to the faster signals, the ENE remains instead about unchanged with the new electronics (red circles).

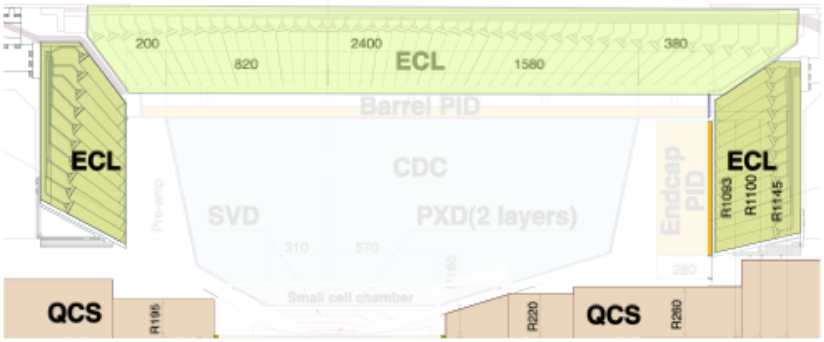

Figure 13: The Belle II electromagnetic calorimeter.

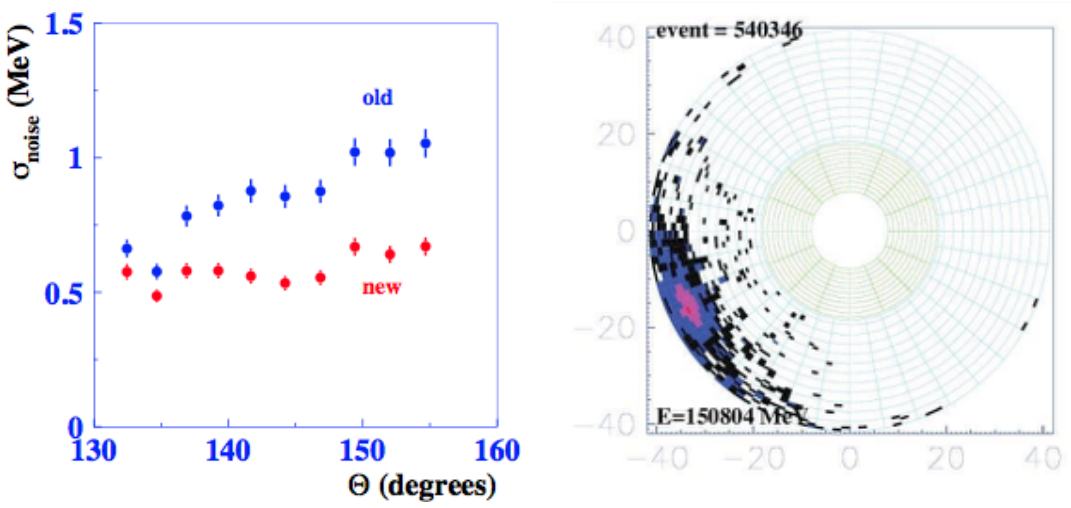

(a) (b)

Figure 14: (a) Plot of the equivalent noise energy in MeV as a function of the polar angle obtained with early prototypes of the new electronics installed on Belle's ECL backward endcap. The background noise, thus pile-up, increases with the polar angle as the crystals get closer to the beam line. (b) Cosmic ray event showing a high energy shower in the endcap ECL.

Presently the ECL's backward endcap and barrel sections are both installed on the detector taking cosmic ray data (see Fig. 14(b)), whereas the forward endcap is fully instrumented and ready to be installed.

3.5 K_L and muon detector: KLM

The outermost Belle II sub-detector is dedicated to the identification of high momentum muons and detection of K_L interactions (KLM) [19]. Belle's iron magnet flux return yoke in both the barrel and endcaps was segmented into 4.7 cm thick plates interspersed with active layers instrumented with glass resistive plate chambers (RPC). The same iron structure is used unchanged by the Belle

II detector. The RPC chambers in the endcaps and the first two innermost layers of the barrel have been replaced with 16,800 plastic scintillator bars, read out via wavelength shifting fibers by silicon photo-multipliers (SiPM). This will allow to cope with the higher neutron backgrounds expected at SuperKEKB. The rest of the barrel was left unchanged. The KLM is all installed and is presently under commissioning with cosmic ray data.

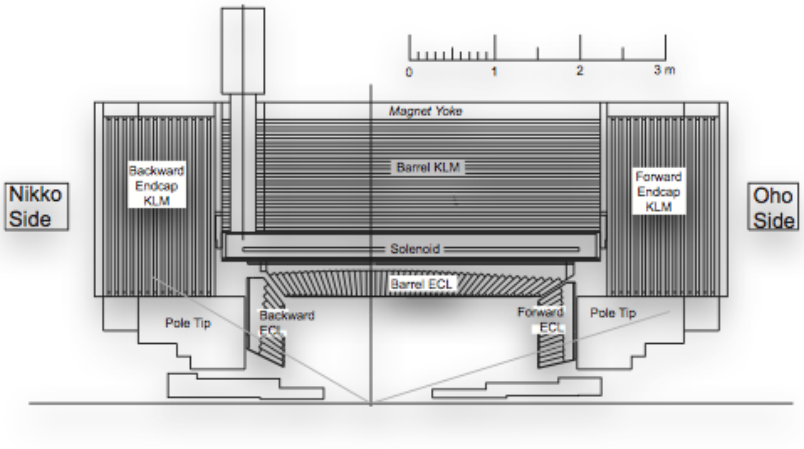

Figure 15: The KLM.

4. Summary and Outlook

In 2016 the SuperKEKB accelerator has successfully completed its first commissioning phase during which the accelerator was turned on for the first time and the two rings have stored currents close to 1 A. During this period the BEAST II background detector system has measured the machine backgrounds, both with coasting beams and during injection.

The construction of the Belle II detector at SuperKEKB is well underway and on schedule. On April 11^{th}, 2017 a major milestone was achieved when Belle II was rolled in the accelerator beam line.

The next steps leading up to the start of the commissioning phase-2 at the end of 2017, are the global cosmic ray run in July and August of 2017 and the installation of the forward endcap A-RICH and ECL in September [1].

At the beginning of 2018 the second commissioning phase will start with Belle II on the beam line without the vertex detector; a five month period leading up to the first beam collisions expected by spring of 2018. The vertex detector will be installed in summer 2018 so that the complete Belle II will be ready for the start of the physics run, foreseen in the Fall of 2018.

References

[1] B. Aubert et al. (*BABAR* Collaboration), NIMA 729 (2013), 615-701, arXiv:1305.3560

[2] A. Abashian et al. (Belle Collaboration) NIMA 479 (2002) 117-232

[1] At the time of writing these proceedings, both these steps have been successfully completed

[3] "The Physics of the B Factories", A. J. Bevan, B. Golob, et al. Eur. Phys. J. C74 (2014) 3026, arXiv:1406.6311

[4] J.P. Lees et al. (*BABAR* Collaboration), Phys. Rev. D 88, 072012 (2013)

[5] Y. Sato et al. (Belle Collaboration), Phys. Rev. D 94, 072007 (2016)

[6] J. P. Lees et al. (*BABAR* Collaboration), Phys. Rev. D 86, 032012

[7] S. Wehle et al. (Belle Collaboration), Phys. Rev. Lett. 118, 111801

[8] R. Aaij et al. (LHCb Collaboration), Phys. Rev. Lett. 115, 111803 (2015)

[9] R. Aaij et al. (LHCb Collaboration), arXiv:1705.05802

[10] T. Abe *et al.* [Belle-II Collaboration], "Belle II Technical Design Report," arXiv:1011.0352 [physics.ins-det]. (2010)

[11] Y. Ohnishi *et al.*, "Accelerator design at SuperKEKB," PTEP **2013**, 03A011 (2013).

[12] M. Baszczyk et al. (SuperB Collaboration), INFN-13-01-PI, LAL-13-01, SLAC-R-1003, arXiv:1306.5655

[13] "The Belle II Pixel Detector for the SuperKEKB Flavour Factory" Proceedings, 23rd International Workshop on Vertex Detectors (Vertex 2014) Doksy, Czech Republic, September 15-19, 2014, PoS Vertex **2014** (2015).

[14] "The silicon vertex detector of the Belle II experiment," K. Adamczyk *et al.* [Belle-IISVD Collaboration], Nucl. Instrum. Meth. A **824**, 406 (2016).

[15] "Central Drift Chamber for Belle-II," N. Taniguchi [Belle II Collaboration], JINST **12**, no. 06, C06014 (2017).

[16] "TOP counter for particle identification at the Belle II experiment" Belle-II PID Group (Kenji Inami (Nagoya U.) for the collaboration). Nucl.Instrum.Meth. A766 (2014) 5-8

[17] "ARICH for Belle II" Y. Yusa (Niigata U.) for the Belle-II Collaboration. JINST 9 (2014) no.10, C10015

[18] "Upgrade of the electromagnetic calorimeter for Belle-II" Kuzmin, A. for the Belle-II ECL group. Proceedings, International Conference on Calorimetry for the High Energy Frontier (CHEF 2013), April 22-25, 2013 p. 83-89.

[19] "K-long and muon system for the Belle II experiment," T. Uglov, JINST **12**, no. 07, C07035 (2017).